

SYNTHESIS, CHARACTERIZATION AND CORROSION INHIBITION SCREENING OF Co(II) DITHIOCARBAMATE COMPLEXES: Co[BuMedtc]₂ AND Co[EtBenzdte]₂

Nur Zalin Khaleda Razali, Muhammad Faiz Abd Latif, Sheikh Ahmad Izaddin Sheikh Mohd Ghazali, Nur Nadia Dzulkifli*

*School of Chemistry and Environment, Faculty of Applied Sciences
Universiti Teknologi MARA (UiTM), Negeri Sembilan Branch, Kuala Pilah Campus, 72000 Kuala Pilah, Negeri Sembilan,
Malaysia*

*Corresponding author: nurnadia@uitm.edu.my

Abstract

Mild steel is a type of carbon steel with quite a low carbon content, or particularly known as plain-carbon steel. It is often used as a construction material because of its relatively low price. However, unlike stainless steel, it has low corrosion resistance, therefore some form of protective film should be applied to prevent it from rusting in corrosive environment. The inhibiting action of the synthesized dithiocarbamates (DTC), namely, Co(II) *N*-butylmethylthiocarbamate, Co[BuMedtc]₂ and Co(II) *N*-ethylbenzylthiocarbamate, Co[EtBenzdte]₂ towards the corrosion behavior of mild steel in acidic solution was studied. The proposed structures of complexes were characterized by using Fourier transform infrared (FTIR), ultraviolet-visible (UV-Vis), gravimetric analysis, molar conductivity, and melting point measurement. The analyses data deduced that the DTC ligands have successfully coordinated to Co(II) ion in a bidentate manner. The corrosion inhibition study showed that Co[BuMedtc]₂ was a better corrosion inhibitor as compared to Co[EtBenzdte]₂ because this is most likely due to the presence of a less bulky alkyl substituent (-CH₃) in Cu[BuMedtc]₂ and hence, showing great corrosion inhibition performance. Besides, the shorter the alkyl chain length in Cu[BuMedtc]₂, the higher the solubility of the complex in the acid medium. The complexes showed better effectiveness in hydrochloric acid (HCl) rather than sulphuric acid (H₂SO₄) solution. The corrosion happened more actively in HCl than H₂SO₄ due to the chloride ions showing more destructive effect than sulfate ion on the carburized low carbon steel samples. In addition, when the concentration of inhibitor increases, the corrosion rate will decrease.

Keywords: Dithiocarbamate, Corrosion, HCl, H₂SO₄, Weight Loss

Article History:- Received: 27 August 2021; Accepted: 14 March 2022; Published: 30 April 2022
© by Universiti Teknologi MARA, Cawangan Negeri Sembilan, 2022, e-ISSN: 2289-6368

Introduction

Corrosion process is a slow but continuous deterioration of metals by the action of the surrounding media such as air, water or salt solution as a result of electrochemical reactions (Nadira et al., 2019). The corrosion process occurs on electrochemical cells, whereby the electrons flow through metal from sites where anodic reactions are going to take place towards the sites which cathodic reactions are taking place. These cell reactions are the results of a pair of anodic and cathodic reactions occurring at the same time on the corroding surface (Aslam et al., 2022). It negatively impacts both natural and industrial environments. Metallic corrosion is the most common problem in industries that leads to huge financial losses to repair and replace corroded materials (Junaedi et al., 2013). Besides, it can also cause pollution to the environment as it releases hazardous waste, especially that from mild steel corrosion which contaminates the air and water (Andreani et al., 2016). Corrosion of mild steel in industries always occurs due to exposure to acids such as hydrochloric acid (HCl), sulfuric acid (H₂SO₄) and in acid cleaning applications (Hashim et al., 2020). The most common activities include the use of an acid solution to remove undesirable scale and rust in the pickling of steel. The use of acid solution causes

metal dissolution and promotes the corrosion process. Hence, the corrosion inhibitor is the most efficient and practical method of protection on a metal surface that is being used to overcome the problem (Yuan et al., 2020). Corrosion inhibitor is a chemical substance that is added to the electrolyte in a small amount to lessen the corrosion rate. It will reduce the rate of both anodic oxidation as well as cathodic reduction by forming a protective layer on the surface of the metal. A study from Chigondo and Chigondo (2016) has shown that most of the previous corrosion inhibitors are inorganic inhibitors that contain phosphate, chromate, and other heavy metals. Recently, it is being slowly prohibited by regulations because of its toxicity, where it has become a threat to aquatic life in the marine industry (Yuan et al., 2020). Moreover, Sanni et al. (2019) also further reported that synthetic organic inhibitors usage is now being harmed due to their toxicity in nature and requires high cost to produce it. Even though compounds such as acetylenic alcohols are used as an effective commercial acidizing inhibitor, it produces toxic vapors under the acidizing process conditions in which it will become a threat to the environment in handling the waste disposal (Quraishi et al., 2002). Most of the effective corrosion inhibitors are the organic inhibitors because it contains heteroatoms like sulfur (S), nitrogen (N), and oxygen (O) having free lone pair of electrons with the presence of aromatic ring in the structure (Li et al., 2019). This allows the capability of the inhibitor to coordinate with the metal substrates via chemisorption mechanism in which it involves the transfer of electrons from inhibitor to the metal (Sastri, 2014). It is significant to search for corrosion inhibitor that is efficient and easily available. Moreover, it should be lower in terms of the cost of production and its toxicity (Aslam et al., 2022).

Dithiocarbamates (DTC) have showed many coordination modes such as isobidentate, anisobidentate, monodentate, and triconnective (Sivasekar et al., 2015). It is an organosulfur ligand that capable of forming complexes with most of the elements and can stabilize transition metals in a variety of oxidation states (Hogarth, 2012). It is by the reason of the resonance forms of dithiocarbamate ligands whereby it is the outcome of delocalization of the nitrogen lone pairs onto the sulfur atom. Scientific interest in complexes with dithiocarbamate anions, $RR'NC(S)(S)^-$ is due to the presence of thioketone and thiol sulfur atoms in those ligands, capable of acting as σ -, π -, or (σ,π) -donor as well as π -acceptor. (Khitrich et al., 2014). In this study, two new series of DTC complexes were synthesized by using in situ method, namely Co(II) *N*-butylmethyldithiocarbamate ($Co[BuMedtc]_2$) and Co(II) *N*-ethylbenzylidithiocarbamate ($Co[EtBenzdct]_2$) complexes. The chelating property of dithiocarbamates are due to their possession of two sulfur atoms which is more effective than nitrogen or oxygen atoms in donating electrons in the ligands (Odularu & Ajibade, 2019). Both complexes were characterized by using the Fourier transform infrared (FTIR) and ultraviolet-visible (UV-Vis) spectroscopy. The melting point for both complexes was recorded and the percentage of Co(II) was studied by using gravimetric analysis. Molar conductivity measurement was also conducted on both complexes. Meanwhile, the corrosion inhibition of different inhibitor concentrations in HCl and H₂SO₄ was determined by using the weight loss method.

Methods

Instrumentation

The infrared spectra were recorded on Perkin Elmer Spectrophotometer, a Fourier Transform-Infrared Attenuated Total Reflectance (FTIR-ATR) in the range of 4000 cm^{-1} – 650 cm^{-1} for mid-IR. The electronic spectra were measured by PG instrument T80/T80+ spectrophotometer in the region of 200 nm – 600 nm for the synthesis complexes using methanol as a solvent. The measurement was conducted using 1 cm quartz cuvettes with 1×10^{-5} M concentration of complexes. The synthesis complexes also undergo determination of melting point using melting point apparatus model SMP10 Stuart and the measurement was taken in an open capillary tube. Furthermore, gravimetric analysis was performed on the Model Lindberg/Blue muffle furnace. The molar conductivity values were measured with DMF solvent at room temperature using SI Analytic Lab 970 conductivity meter at the concentration of 2×10^{-3} M.

Synthesis of Co(II) dithiocarbamate complexes

The complex of Co[BuMedtc]₂, with the molar ratio of reaction materials is 2:2:1. An ethanolic solution of *N*-butylmethylamine (0.002 mol) was stirred for one hour at 4°C before adding an ethanolic solution of carbon disulfide (0.002 mol). After 30 minutes, a few drops of ammonia were added to the mixture until precipitate began to form. Thereafter, 10 mL of cobalt(II) chloride (0.001 mol) solution was added into the mixture and stirred for 2 hours. The color precipitate formed. The mixture then was filtered, washed with cold ethanol and dried. The product was recrystallized by using acetonitrile:tetrahydrofuran (1:2) mixture. The product purity was checked by a thin-layer chromatography (TLC). The steps were repeated to synthesize Co[EtBenzdte]₂ with *N*-ethylbenzylamine as the starting material (Sonia & Bhaskaran, 2017).

Corrosion Inhibition Study

The acidic solution 1 M of 37 % of HCl was prepared by a dilution process. The inhibitor concentrations were 0.1, 0.01 and 0.001 M in which were diluted with 1 M of HCl and H₂SO₄ solution. The mild steel with size of 4 x 1.5 cm was cleaned by using emery paper and washed with distilled water and acetone. After that, the initial weight of dried and cleaned mild steel was measured using an analytical balance. Next, the specimens were immersed in 10 mL of 1 M HCl solution with and without different inhibitor concentrations at room temperature. After 24 hours of immersion, the specimen was rinsed with distilled water and then dried. The final weight of specimens was recorded and average mass was calculated. The corrosion inhibition activity was repeated to replace HCl with H₂SO₄. The experiment was performed in triplicate to determine the average weight. The weight loss of mild steel, ΔW(g), the corrosion rate C_{RW} (mg cm⁻² h⁻¹), surface coverage (θ) and inhibition efficiency, IE_{WL}(%) can be calculated as shown in Equation (1) to Equation (4), respectively (Daoud et al., 2015).

$$\Delta W = W_1 - W_2 \quad (1)$$

$$C_{RW} = \frac{\Delta W}{St} \quad (2)$$

$$\theta = \frac{C_{RW}^{\circ} - C_{RW}}{C_{RW}^{\circ}} \quad (3)$$

$$IE_{WL} = \left(\frac{C_{RW}^{\circ} - C_{RW}}{C_{RW}^{\circ}} \right) \times 100 \quad (4)$$

Where:-

W₁ = the average weight of mild steel before immersion (g)

W₂ = the average weight of mild steel after immersion (g)

ΔW = the average weight loss (g)

S = the surface area of mild steel (cm²)

t = the immersion time (h)

C_{RW}^o = the corrosion rate in the absence of the inhibitor

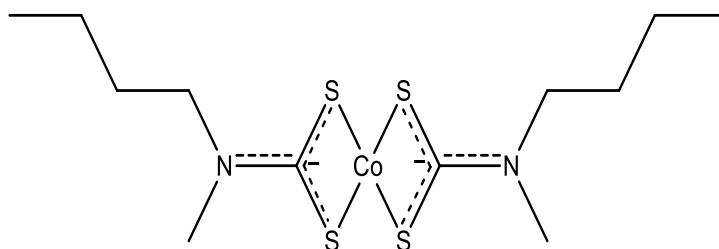
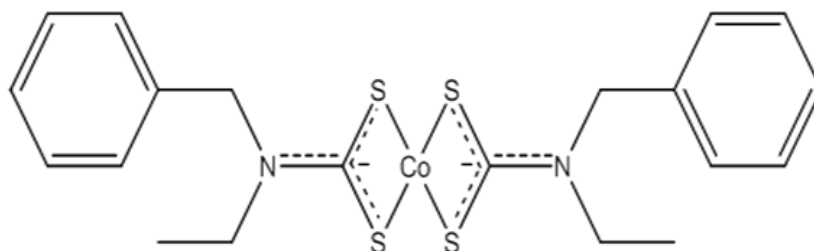
C_{RW} = the corrosion rate in the presence of the inhibitor

IE_{WL} = inhibitor efficiency

Result and Discussion

Synthesis of Co[BuMedtc]₂ and Co[EtBenzdte]₂

The synthesis of Co[BuMedtc]₂ complex with a molar ratio of 2:2:1 yielded dark green color precipitate while synthesis of Co[EtBenzdte]₂ complex yielded light green color precipitate. The complexes showed different types of colors due to the properties of ligands used. Synthesis was carried out using a condensation method aimed to prepare dithiocarbamate complexes through in situ synthesis. The melting point for both complexes was found at 360°C to 375°C. The difference values of melting point in the range 1°C – 3°C indicated the complexes were relatively free of impurities. Figure 1 and Figure 2 show the proposed structures for both complexes of Co[BuMedtc]₂ and Co[EtBenzdte]₂, respectively.

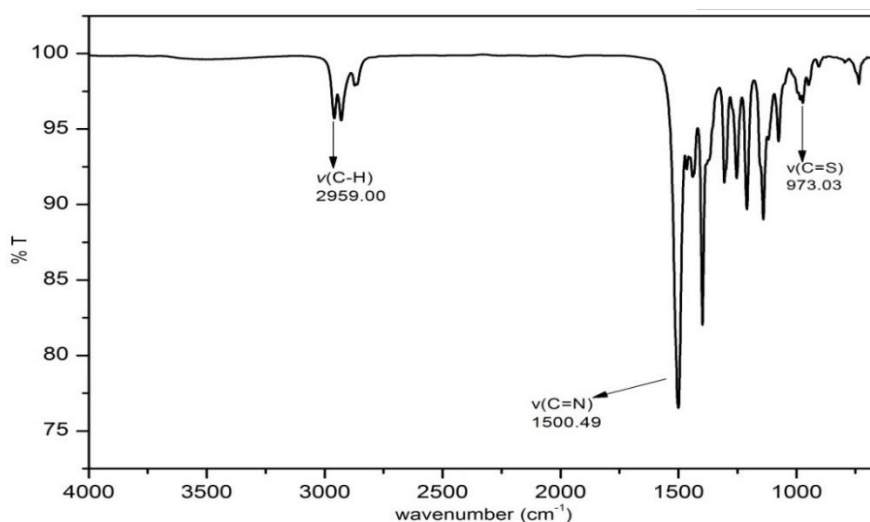
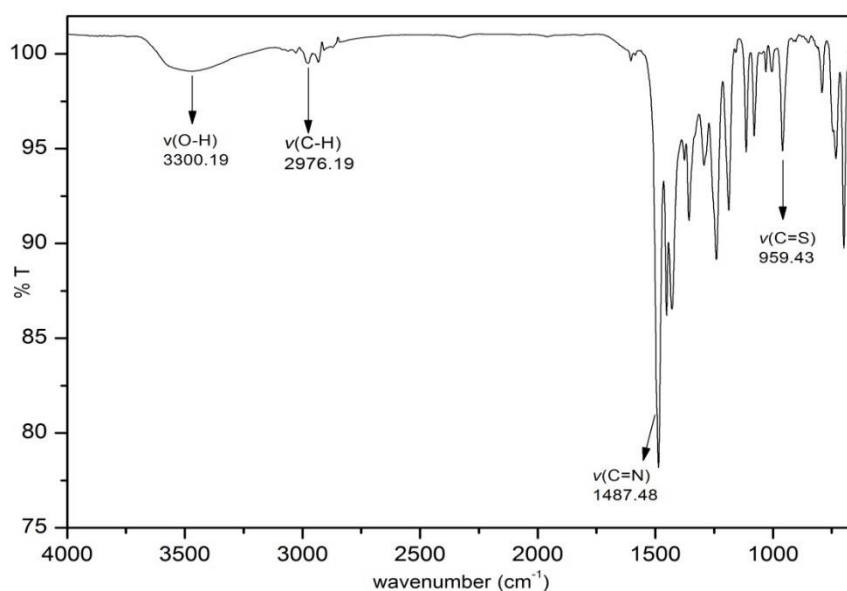
Figure 1. Proposed structure for Co(II) *N*-butylmethyldithiocarbamate, Co[BuMedtc]₂.Figure 2. Proposed structure for Co(II) *N*-ethylbenzylidithiocarbamate, Co[EtBenzdtc]₂.

Fourier Transform-Infrared Attenuated Total Reflectance (FTIR-ATR) Spectroscopy

Table 1 comprises the FTIR-ATR data obtained for Co[BuMedtc]₂, Co[EtBenzdtc]₂, and their starting materials. Two important stretching bands were observed for both complexes, which were $\nu(\text{C}=\text{S})$ and $\nu(\text{C}=\text{N})$. The complexes spectra notified that the stretching band of thioureide moiety, $\nu(\text{C}=\text{N})$ shows partial double bond characteristic due to the electron delocalization within dithiocarbamate (Awang et al., 2010) with the value of 1500 cm^{-1} for Co[BuMedtc]₂ and 1487 cm^{-1} for Co[EtBenzdtc]₂. The presence of $\nu(\text{C}=\text{N})$ and $\nu(\text{C}=\text{S})$ have confirmed the structures of dithiocarbamate complexes. Table 1 reveals that the stretching band of $\nu(\text{C}=\text{S})$ for Co[BuMedtc]₂ and Co[EtBenzdtc]₂ is 973 cm^{-1} and 959 cm^{-1} , respectively. This suggestion based on the chelating character of the dithiocarbamate moiety to Co(II) ion (Brown et al., 1976). The $\nu(\text{C}=\text{S})$ stretching vibration was detected at approximately 1000 cm^{-1} without any splitting suggesting a bidentate nature of the dithiocarbamate ligand. Shahzadi et al. (2007) observed that $\nu(\text{C-N})$ vibrations lie between the range 1250 cm^{-1} - 1360 cm^{-1} for C-N single bonds and 1640 cm^{-1} - 1690 cm^{-1} for C-N double bonds. The $\nu(\text{C}=\text{N})$ stretching band in both complexes showed a higher wavenumber compared to $\nu(\text{C-N})$ in butylmethylamine (1460 cm^{-1}) and ethylbenzylamine (1454 cm^{-1}). This happened due to the delocalization of electrons towards the center of the metal after being coordinated with DTC ligands. Furthermore, there was a broad peak that appeared at 3300 cm^{-1} corresponding to $\nu(\text{O-H})$ vibration in Co[EtBenzdtc]₂. This was probably because the complex was not dried enough and needed a longer time to be fully dried.

Table 1. Summary of FTIR-ATR data for Co[BuMedtc]₂ and Co[EtBenzdtc]₂ and their starting materials.

Compounds	Wavenumber (cm ⁻¹)						
	$\nu(\text{C-N})$	$\nu(\text{C-H})$	$\nu(\text{C=S})$	$\nu(\text{N-H})$	$\nu(\text{C}=\text{S})$	$\nu(\text{C}=\text{N})$	$\nu(\text{O-H})$
Carbon disulfide	-	-	1541	-	-	-	-
Butylmethylamine	1460	2959	-	3408	-	-	-
Ethylbenzylamine	1454	2966	-	3305	-	-	-
Co[BuMedtc] ₂	-	2959	-	-	973	1500	-
Co[EtBenzdtc] ₂	-	2976	-	-	959	1487	3300

Figure 3. IR spectrum of Complex Co[BuMedtc]₂, C1.Figure 4. IR spectrum of Complex Co[EtBenzdte]₂, C2.

UV-Vis Spectroscopy

The electronic transition spectra data of Co[BuMedtc]₂ and Co[EtBenzdte]₂ had been displayed in Table 2. A transition of $\pi \rightarrow \pi^*$ at 220 nm represented S-C=S in carbon disulfide, CS₂. Meanwhile, both complexes displayed an absorption peak at 270 nm, implying the $\pi \rightarrow \pi^*$ transition in N-C=S and S-C=S. Dithiocarbamates usually show two absorption peaks in the UV indicating to the $\pi \rightarrow \pi^*$ and $n \rightarrow \pi^*$ transitions (Mamba et al., 2010). Coordination of dithiocarbamate to the Co(II) led to changes in the spectra region. The change in the ligand conjugation was caused by the deprotonation of the ligand upon coordination. The $n \rightarrow \pi^*$ transition were also present in the spectra of the complexes with small shifting which were assigned 325 nm for both Co[BuMedtc]₂ and Co[EtBenzdte]₂. The presence of absorption peak at 480 nm for Co[BuMedtc]₂ and 475 nm for Co[EtBenzdte]₂ were due to $d-d$ transitions in accordance with the d^7 electron configuration of Co(II) ion. The number of unpaired electrons for Co(II) that was obtained was based on electron configuration [Ar] $3d^7$ and the electron arrangement in the free ion of the metal.

Table 2. Electronic spectra data for the raw material and its metal complexes.

Compounds	Transitions	λ_{\max} (nm)	Molar absorptivity, ϵ ($M^{-1} \text{ cm}^{-1}$)
Carbon disulfide	$n \rightarrow \pi^*$	295	13300
	$\pi \rightarrow \pi^*$	220	167100
Co[BuMedtc] ₂	$n \rightarrow \pi^*$	325	134500
	$\pi \rightarrow \pi^*$	270	192100
	$d-d$	480	2300
Co[EtBenzdte] ₂	$n \rightarrow \pi^*$	325	122400
	$\pi \rightarrow \pi^*$	270	182300
	$d-d$	475	1900

The bathochromic shifting of the transition was due to the complexation effect of the metal ions (Ali et al., 2013). The bands related to $\pi \rightarrow \pi^*$ electronic transition in the complexes shifted compared with those observed at the free Schiff base ligands. This referred to the coordination of the ligands to the metal center of the complexes (Mahmoud et al., 2020). It involves the shift of absorption maximum towards higher wavelength in the complexes due to the presence of a certain functional group on the ligands. The molar absorptivity, ϵ shows the ability of complexes to absorb light at a certain wavelength. There was absorption occurring at a range higher than 400 nm, which represented the $d-d$ transition (Latif et al., 2018). This portrayed the lower value of molar absorptivity for $d-d$ transitions, which was $2300 \text{ M}^{-1} \text{ cm}^{-1}$ for Co[BuMedtc]₂ and $1900 \text{ M}^{-1} \text{ cm}^{-1}$ for Co[EtBenzdte]₂.

Gravimetric Analysis

The gravimetric analysis of Co(II) was carried out within a temperature range above room temperature up to $30 \text{ }^\circ\text{C}$ (Aslam et al., 2020). This analysis was conducted to determine the mass (by percentage) of metal in the complexes. The solid residue which was cobalt oxides, CoO formed after the decomposition was completed. The percentage of metal calculated for Co[BuMedtc]₂ and Co[EtBenzdte]₂ were 7.59% and 4.33%, respectively. The equations shown below were used to determine the percentage of metal in both complexes, whereby a refers to mole of analyte while b is mole of precipitate.

$$\text{Gravimetric Factor, GF} = \frac{\text{Molecular weight of analyte}}{\text{Molecular weight of precipitate}} \times a/b$$

$$\text{Weight of analyte} = \text{Weight of precipitate} \times \text{GF}$$

$$\text{Percentage of analyte (\%)} = \frac{\text{Weight of analyte}}{\text{Weight of precipitate}} \times 100$$

Molar Conductivity Measurement

The molar conductivity of both Co(II) complexes lie in the range $4.0 \text{ S cm}^2 \text{ mol}^{-1}$ – $12.5 \text{ S cm}^2 \text{ mol}^{-1}$ indicating non-electrolyte behavior (Hazani et al., 2018). Moreover, the deduced data indicated that there were no counter ions present in the complexes. The non-electrolyte behavior shows that the ligand was directly coordinated to the central Co(II) (Jyothi & Farook, 2019).

Corrosion Inhibition Study

The corrosion inhibition activity was carried out on mild steel in 1 M HCl and H₂SO₄ solution using the weight loss method. This study aims to compare the effect of complexation and substituent groups present in the inhibitors on the corrosion inhibition performance for the mild steel in an acidic medium. The mild steels were submerged for 24 hours at room temperature in varying acid concentrations. The

variety concentration of 0.001 M, 0.01 M, and 0.1 M were chosen to identify the effectiveness of the inhibitor's concentration towards the corrosion rate. The corrosion inhibitor data can be shown below in Table 3. The investigated ligands were chosen based on the effect of alkyl substituents present in the structures. The inhibitor efficiency tends to increase as inhibitor concentration increases. It is also noteworthy that the Co[BuMedtc]_2 complex at 0.1 M of inhibitor concentration shows good inhibition efficiency for mild steel in 1 M hydrochloric acid and 1 M sulphuric acid as compared to Co[EtBenzdte]_2 complex. This was most likely due to the presence of less bulky alkyl substituent ($-\text{CH}_3$) in Co[BuMedtc]_2 . Meanwhile, a bulkier group in Co[EtBenzdte]_2 tends to cause a steric hindrance that affects the orientation of inhibitor molecules on the metal surfaces and reduces their corrosion inhibition effectiveness (Blagus & Kaitner, 2010). Co[EtBenzdte]_2 has a high electron releasing effect on its ligand compared to the ligand in Co[BuMedtc]_2 . This was due to the presence of ethyl group ($-\text{CH}_2\text{-CH}_3$) in Co[EtBenzdte]_2 structure and methyl group ($-\text{CH}_3$) in Co[BuMedtc]_2 . Shetty (2019) has stated that the presence of multiple electron releasing groups shows stronger adsorption onto a metal surface and exhibits good inhibition activity. Thus, a ligand from Co[EtBenzdte]_2 will be more favored to be adsorbed on the metal surface than Co[BuMedtc]_2 as it can penetrate easily to the aqueous phase. It is also chemically adsorbant at the metal/solution interface (Aiad & Negm, 2009). Besides, this also indicated that more complexes were adsorbed on the metal surface when the inhibitor concentration increases, promoting wider surface coverage and these complexes act as chemisorption inhibitors. The efficiency of the complexes as corrosion inhibitors depends on their ability to be adsorbed onto the metal surface. In this study, the corrosion rate of complexes in H_2SO_4 was higher than HCl medium as shown in Table 3.

Focusing on Co[BuMedtc]_2 , H_2SO_4 has a higher corrosion rate due to its efficiency to ionize completely in the solution by emitting two mole of protons. Hence, it can react strongly to the surface of mild steel compared to HCl in which it only emits one proton. According to Loto (2018), oxide film formation occurs faster in H_2SO_4 than HCl solution, resulting in greater pores emerging on the surface of mild steel, thereby higher corrosion rate. Ouakki et al.(2019) also emphasized that sulfuric acid corrodes mild steel and makes the surface of metal highly asymmetrical. However, it can be seen from the analysis of Co[EtBenzdte]_2 that the highest inhibition efficiency was recorded at 0.1 M H_2SO_4 . This was probably due to the chloride ions that have shown more destructive effect than sulfate ion, hence the corrosion happened more actively in HCl than H_2SO_4 (Ajeel et al., 2012). From Figure 5, it can be concluded that the inhibitor efficiency increases as the inhibitor concentration increases. Overall, Co[BuMedtc]_2 shows better inhibition efficiency than Co[EtBenzdte]_2 . Moreover, it shows that the corrosion rate decreases as the inhibitor concentration increases as shown in Figure 6. Inhibitor at concentration 0.001 M corrodes at a higher rate and Co[EtBenzdte]_2 shows high corrosion rate over 24 hours immersion time as compared to Co[BuMedtc]_2 (Daoud et al., 2015; Othman et al., 2021).

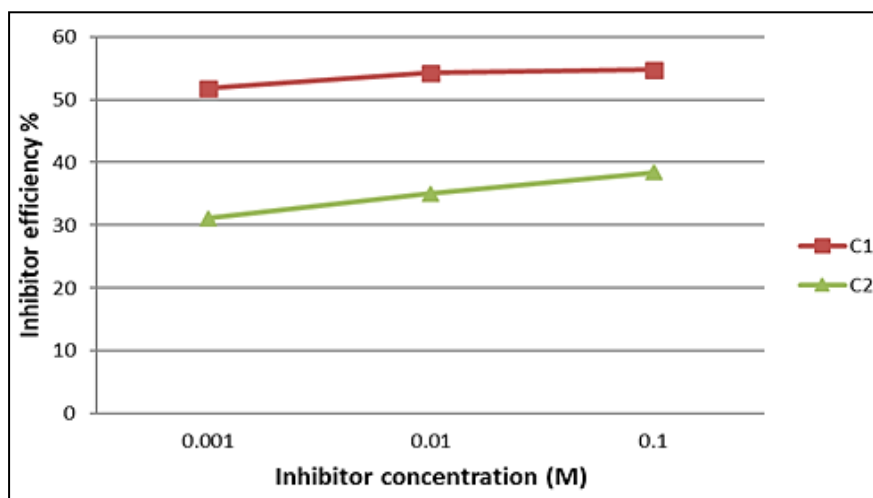


Figure 5. Inhibitor efficiency for Co[BuMedtc]_2 (C1) and Co[EtBenzdte]_2 (C2) in different concentration of HCl.

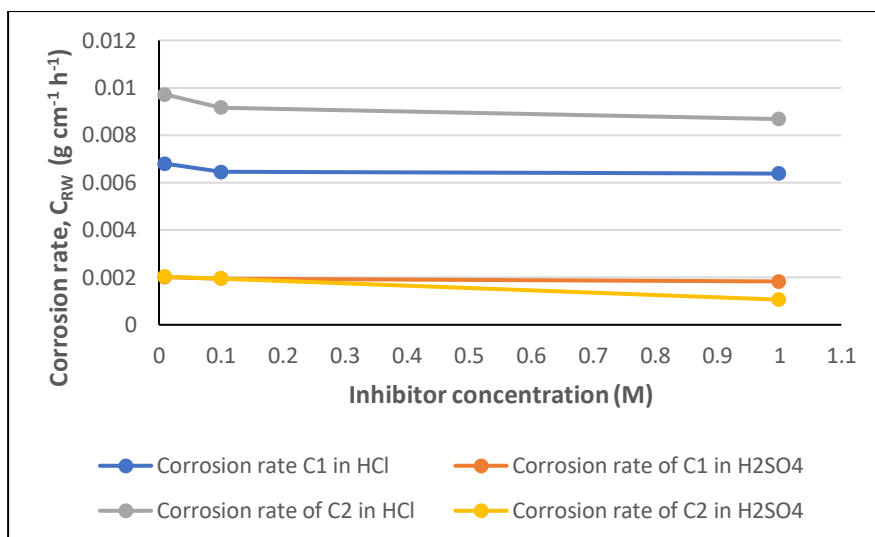


Figure 6. Corrosion rate for Co[BuMedtc]₂ (C1) and Co[EtBenzdte]₂ (C2) in different concentration of HCl and H₂SO₄.

Table 3. The corrosion inhibitor data.

Solution	Inhibitor	Concentration (M)	Weight loss, ΔW (g)	Corrosion rate, C _{RW} (g cm ⁻¹ h ⁻¹)	Inhibitor efficiency, η _w (%)
HCl	Blank	1	0.203	1.41 x 10 ⁻³	-
	Co[BuMedtc] ₂	0.1	0.092	6.38 x 10 ⁻⁴	54.7
		0.01	0.093	6.45 x 10 ⁻⁴	54.25
		0.001	0.098	6.80 x 10 ⁻⁴	51.77
	Co[EtBenzdte] ₂	0.1	0.125	8.68 x 10 ⁻⁴	38.43
		0.01	0.132	9.16 x 10 ⁻⁴	35.03
		0.001	0.140	9.72 x 10 ⁻⁴	31.06
H ₂ SO ₄	Blank	1	0.355	2.46 x 10 ⁻³	-
	Co[BuMedtc] ₂	0.1	0.264	1.83 x 10 ⁻³	25.60
		0.01	0.281	1.95 x 10 ⁻³	20.73
		0.001	0.290	2.01 x 10 ⁻³	18.29
	Co[EtBenzdte] ₂	0.1	0.153	1.06 x 10 ⁻³	56.91
		0.01	0.281	1.95 x 10 ⁻³	20.73
		0.001	0.292	2.03 x 10 ⁻³	17.48

Conclusion

Both Co[BuMedtc]₂ and Cu[EtBenzdte]₂ have been successfully synthesized under condensation reaction and fully characterized by using FTIR-ATR and UV-Vis, melting point determination, gravimetric analysis, and molar conductivity measurement. Both complexes had gone through corrosion inhibition screening and as a result, both Co(II) complexes have potential to be applied as corrosion inhibitors. These complexes demonstrated promising anti-corrosion activity, whereby as the inhibitor concentration increased, the corrosion rate decreased. Overall, Co[BuMedtc]₂ showed good performance as a corrosion inhibitor compared to Co[EtBenzdte]₂ in HCl medium at 0.1 M of inhibitor

concentration with the highest percentage recorded at 54.7%.

Acknowledgement

The authors would like to express their gratitude to the Faculty of Applied Sciences, Universiti Teknologi MARA, Negeri Sembilan Branch, Kuala Pilah Campus, Negeri Sembilan, Malaysia for providing the research facilities.

References

- Aiad, I., & Negm, N. A. (2009). Some corrosion inhibitors based on Schiff base surfactants for mild steel equipments some corrosion inhibitors based on Schiff base surfactants for mild steel equipments. *Journal of Dispersion Science and Technology*, 30(8), 1142–1147.
- Ajeel, S. A., Waadulah, H. M., & Sultan, D. A. (2012). Effects of H₂SO₄ and HCl concentration on the corrosion resistance of protected low carbon steel. *Al-Rafidain Engineering*, 20(6), 70–76.
- Ali, I., Wani, W. A., Saleem, K., & Hseih, M. (2013). Design and synthesis of thalidomide based dithiocarbamate Cu(II), Ni(II) and Ru(III) complexes as anticancer agents. *Polyhedron*, 56, 134–143.
- Andreani, S., Znini, M., Majidi, L., Hammouti, B., Costa, J., & Muselli, A (2016). Study of corrosion inhibition for mild steel in hydrochloric acid solution by *Limbarda crithmoides* (L.) essential oil of corsica. *Journal of Materials and Environmental Science*, 7(1), 187-195.
- Aslam, J., Aslam, R., Alrefaee, S. H., Mobin, M., Aslam, A., Parveen, M., & Mustansar Hussain, C. (2020). Gravimetric, electrochemical, and morphological studies of an isoxazole derivative as corrosion inhibitor for mild steel in 1M HCl. *Arabian Journal of Chemistry*, 13(11), 7744–7758.
- Aslam, R., Serdaroglu, G., Zehra, S., Kumar Verma, D., Aslam, J., Guo, L., Verma, C., Ebenso, E. E., & Quraishi, M. A. (2022). Corrosion inhibition of steel using different families of organic compounds: Past and present progress. *Journal of Molecular Liquids*, 348, 1–29.
- Awang, N., Baba, I., Mohd Yousof, N. S. A., & Kamaludin, N. F. (2010). Synthesis and characterization of organotin(IV) N-benzyl-N-isopropylthiocarbamate compounds: Cytotoxic assay on human hepatocarcinoma cells (HepG2). *American Journal of Applied Sciences*, 7(8), 1047–1052.
- Blagus, A., & Kaitner, B. (2010). Schiff base in the Cambridge Structural Database (CSD). *Macedonian Journal of Chemistry and Chemical Engineering*, 29(2), 117–138.
- Brown, D. A., Glass, W. K., & Burke, M. A. (1976). The general use of IR spectral criteria in discussions of the bonding and structure of metal dithiocarbamates. *Spectrochimica Acta Part A: Molecular Spectroscopy*, 32(1), 145–147.
- Chigondo, M., & Chigondo, F. (2016). Recent natural corrosion inhibitors for mild steel : An overview. *Journal of Chemistry*, 2016.
- Daoud, D., Douadi, T., Hamani, H., Chafaa, S., & Al-Noaimi, M. (2015). Corrosion inhibition of mild steel by two new S-heterocyclic compounds in 1 M HCl : Experimental and computational study. *Corrosion Science*, 94, 21-37.
- Hashim, N. Z., Kahar, M. A., Kassim, K., Embong, Z., & Anouar, E. H. (2020). Experimental and theoretical studies of azomethines derived from benzylamine as corrosion inhibitors of mild steel in 1 M HCl. *Journal of Molecular Structure*, 1222(2020), 1–13.
- Hazani, N. N., Dzulkifli, N. N., Ghazali, S. A. I. S. M., Mohd, Y., Farina, Y., & Ngatiman, F. (2018). Synthesis, characterization and effect of temperature on corrosion inhibition by thiosemicarbazone derivatives and its tin (IV) complexes. *Malaysian Journal of Analytical Sciences*, 22(5), 758–767.
- Hogarth, G. (2012). Metal-dithiocarbamate complexes : Chemistry and biological activity. *Mini-Reviews in Medicinal Chemistry*, 12, 1202–1215.

Junaedi, S., Al-Amiery, A., Kadhum, A., Kadhum, A., & Mohamad, A. (2013). Inhibition effects of a synthesized novel 4-aminoantipyrine derivative on the corrosion of mild steel in hydrochloric acid solution together with quantum chemical studies. *International Journal of Molecular Sciences*, 14(6), 915–928.

Jyothi, N. R., & Farook, N. A. M. (2019). Synthesis and characterization of newly synthesized thiosemicarbazone ligands with IR, NMR and mass spectral techniques. *Oriental Journal of Chemistry*, 35(1), 43–47.

Khitrich, N. V., Vlasenko, V. G., Seifullina, I. I., & Zubavichus, Y. V. (2014). Local surrounding of Cobalt (II) in dithiocarbamate complexes, their magnetic and spectral properties. *Russian Journal of General Chemistry*, 84(3), 555–561.

Latif, H., Ahmad, S., Sheikh, I., Ghazali, M., Abdullah, E. N., Lahuri, A. H., Ngatiman, M. F., & Dzulkifli, N. N. (2018). Synthesis, structural, density functional theory, and x-ray diffraction study of Zn (II) N-isopropylbenzylidithiocarbamate: Anti-corrosion screening in acid media. *Indonesian Journal of Chemistry*, 18(4), 755–765.

Li, F., Bai, M., Wei, S., Jin, S., & Shen, W. (2019). Multidimension insight involving experimental and in silico investigation into the corrosion inhibition of N, N - dibenzyl dithiocarbamate acid on copper in sulfuric acid solution. *Industrial & Engineering Chemistry Research*, 58, 7166–7178.

Loto, R. T. (2018). Surface coverage and corrosion inhibition effect of *Rosmarinus officinalis* and zinc oxide on the electrochemical performance of low carbon steel in dilute acid solutions. *Results in Physics*, 8, 172–179.

Mahmoud, W. A., Ali, Z. M. H., & W., R. (2020). Synthesis and spectral analysis of some metal complexes with mixed mixed Schiff base ligands 1- [2- (2-hydroxybenzylideneamino)ethyl]pyrrolidine-2,5-dione (HL1) and (2-hydroxybenzalidine)glycine (HL2). *Journal of Physics: Conference Series*.

Mamba, S. M., Mishra, A. K., Mamba, B. B., Njobeh, P. B., Dutton, M. F., & Fosso-Kankeu, E. (2010). Spectral, thermal and in vitro antimicrobial studies of cyclohexylamine-N-dithiocarbamate transition metal complexes. *Spectrochimica Acta - Part A: Molecular and Biomolecular Spectroscopy*, 77(3), 579–587.

Nadira, N., Mohd, Y., Ahmad, S., Sheikh, I., & Ghazali, M. (2019). Electrochemical studies of thiosemicarbazone derivatives and its tin (IV) complex as corrosion inhibitor for mild steel in 1 M hydrochloric acid. *Chemistry Journal of Moldova*, 14(1), 98–106.

Odularu, A. T., & Ajibade, P. A. (2019). Dithiocarbamates : Challenges, control, and approaches to excellent yield, characterization, and their biological applications. *Bioinorganic Chemistry and Applications*, 2019, 15.

Othman, N. F. H., Latif, N. S. H., Ghazali, S. A. I. S. M. Abdullah, E. N., & Dzulkifli, N. N. (2021). Ni(II) Butylmethyldithiocarbamate: PhysicoChemical Properties, X-Ray Crystallography, DFT and Anti-Corrosion Screening in Different Acids. *ASM Science Journal*, 16, 1-11.

Ouakki, M., Galai, M., Rbaa, M., Abousalem, A. S., Lakhri, B., & Cherkaoui, M. (2019). Quantum chemical and experimental evaluation of the inhibitory action of two imidazole derivatives on mild steel corrosion in sulphuric acid medium. *Heliyon*, 5, e02759.

Quraishi, M. A., Sardar, N., & Ali, H. (2002). A study of some new acidizing inhibitors on corrosion of N-80 alloy in 15 % boiling hydrochloric acid. *Corrosion Science*, 58(4), 317–321.

Shahzadi, S., Ali, S., Wurst, K., & Najam-ul-haq, M. (2007). Synthesis of stannic (IV) complexes : Their structural elucidation in solid and solution state and antimicrobial activity. *Heteroatom Chemistry*, 18(6), 664–674.

Shetty, P. (2019). Schiff bases : An overview of their corrosion inhibition activity in acid media against mild steel against mild steel. *Chemical Engineering Communications*, 0(0), 1–45.

Sivasekar, S., Ramalingam, K., & Rizzoli, C. (2015). Metal dithiocarbamate precursors for the preparation of a binary sulfide and a pyrochlore : Synthesis, structure, continuous shape measure and bond valence sum analysis of antimony (III) dithiocarbamates. *Polyhedron*, 85, 598–606.

Sanni, O., Fayomi, O., & Popoola, A. (2019). Eco-friendly inhibitors for corrosion protection of stainless steel: An overview. *Journal of Physics: Conference Series*, 1378(4), 42-47.

Sastri, V. S. (2014). *Types of corrosion inhibitor for managing corrosion in underground pipelines. in underground pipeline corrosion: Detection, analysis and prevention*. Woodhead Publishing Limited: pp. 166–211.

Sonia, A. S., & Bhaskaran, R. (2017). Tris dithiocarbamate of Co(III) complexes: Synthesis, characterization, thermal decomposition studies and experimental and theoretical studies on their crystal structures. *Journal of Molecular Structure*, 1134, 416–425.

Yuan, Q., Cheng, R., Zou, S., Ding, C., Liu, H., Wang, Y., Yang, D., Xiao, X., Jiang, Q., Tang, R., & Chen, J. (2020). Isatin thiosemicarbazone derivatives as inhibitors against corrosion of AA6060 aluminium alloy in acidic chloride medium: substituent effects. *Integrative Medicine Research*, 9(5), 11935–11947.